Mechanical performance and healing process improvement of cement-coir pith particle composites by accelerated carbonation

Franco Josué Amaya Suazo [1], João Domingos Covello Carregosa [2],
Rosane Maria Pessoa Betânio Oliveira [2], Wilson Acchar [3]

[1] Facultad de Ingeniería Mecánica y Eléctrica, Universidad Autónoma de Nuevo León - FIME/UANL, CEP: 66455, San Nicolás de los Garza, NL, Mexico.

[2] Department of Materials Science and Engineering, Federal University of Sergipe - P^{2}CEM/UFS, CEP: 49100-000, São Cristóvão, SE, Brazil.

[3] Phisycs Institut, Federal University of Rio Grande do Norte – FIS/UFRN, CEP: 59078-900, Natal, RN, Brazil.
e-mail: franco.amaya89@gmail.com, jdcovello@hotmail.com, rosaneboliveira@gmail.com, wacchar@gmail.com

ABSTRACT

The accelerated carbonation during the early cure age is a process used to improve the physical and mechanical properties of cement-based composites. In this work, cement-based composites with coir pith particles addition were subjected to the accelerated carbonation process during the first 48 hours of cure in a rich CO_2 environment. After curing, the samples were dried and subjected to curing conditions until saturated at 28 days. Thermogravimetric analyses, scanning electron microscopy (SEM) and X-ray diffraction patterns were used to analyze the impact of accelerated carbonation during the early cure age in cement-coir pith composite. The results of the physical properties show an increase in bulk density and surface density of the carbonated samples, as well as reduced water absorption. The reduction of the $Ca(OH)_2$ resulting in the increasing of $CaCO_3$ content was observed by thermogravimetric analysis. The carbonated samples had a 41% increase in compression strength and 28% in the modulus of rupture as compared to non-carbonate samples. The results showed the potential of the accelerated carbonation cure process in cement-based composites with vegetable coconut waste addition.

Keywords: Accelerated carbonation, mechanical properties, thermal analysis, cement-based composites, coir pith particles

1. INTRODUCTION

In recent years, the use of waste of vegetable origin in cement-based composites has increased considerably. However, the vegetal fibers affect the composites durability, when exposed to natural weathering or environmental degradation, due to its chemical composition, its behavior in the alkaline environment of the cement matrix and mineralization through the migration of cement hydration products [1]. Moreover, some studies say that promotes a decrease of the mechanical properties [1,2].

The natural fibers are composed mainly of cellulose, hemicellulose and non-cellulosic materials (lignin, pectin, and wax) [3]. The coconut fiber is considered a lignocellulosic material (37% lignin, 32.5% cellulose and 30.5% hemicellulose) [4]. The lignocellulosic residues have features like; low density, ease of processing and abundant availability of raw materials [5]. The lignocellulosic material has not good compatibility with cement, which is necessary a pre-treatment to fibers or composites, also use of an additive in the mix, another option is the treatment to the cement-based composites in the early cure age like accelerated carbonation. Actually, the coconut industry generates various kinds of sub-products such as; mature coconut husk and coir from the fibrous husk (or mesocarp). In the coir, only 30% is passed to manufacture of fibers that have some textile applications (mats, carpets), construction (thermal insulation) and automobiles (cushions, seat covers), the rest 70% is made up of short fibers and coir pith particle, nowadays these wastes are taken to landfills. In response to environmental demands, some forms of exploitation of these wastes are being studied [6]. These sub-products are mainly used as fertilizer or power generation fuel and have none or little used in the construction industry [4,6].

Currently, carbon emissions reduction is a global solution at a time when the world needs to rapidly

reduce greenhouse gas emissions. Recent studies showed that the organic material into cement matrix sequester CO_2 from the atmosphere more efficiently [7], that property has led to an increase in research in recent years using accelerated carbonation in the processes of curing cement-based materials [8-10].

In cement-based materials, the study of hydration products are affected during the accelerated carbonation process during the early cure age is important. If only calcium hydroxide is carbonated, the porosity could be decreased; however, if calcium-silicate-hydrate (C-S-H) is the main phase attached for the carbonation, the porosity and permeability could be increased considerably [8]. Carbon dioxide could be injected during early age curing to encourage improvements in the vegetable material-cement matrix compatibility. The permeability and carbonation depth could be increased with the coconut fibers content [11], previous investigations showed improved durability of reinforced panels with vegetable sisal and coconut fibers-mortar composites; by immersing the fibers in a silica slurry, and accelerated carbonation at the beginning of curing in an environment rich in CO_2 [12].

Previous studies showed that accelerated carbonation promotes the mechanical properties improvement due to a $Ca(OH)_2$ reduction [12,13]. Cement-based composites reinforced with eucalyptus pulp in curing conditions under atmosphere rich in CO_2 showed improved mechanical properties [1]. In this sense, reduced $Ca(OH)_2$ and increased $CaCO_3$ content produces less porosity, higher density and good fiber-matrix adhesion due to $CaCO_3$ have greater chemical stability, and higher density than the $Ca(OH)_2$ [1].

Carbonation is a relatively slow process and rapid aging of the samples is; this requires the use of accelerated carbonation chamber, with CO_2 levels that exceed those found in real environments, with detailed control of the levels of temperature and relative humidity. The accelerated carbonation treatment was mainly applied in wood-cement panels because this method is more suitable for panels than for blocks, due to the difficult uniform injection of gas into a block. [5].

In this context, this work presents an evaluation of the effect of accelerated carbonation in the early cure age of composite cement-coir pith particle. The samples were subjected to different curing conditions. The curing process influenced the microstructure and in the physical-mechanical properties was investigated. The major products of the process of hydration and carbonation of the cement composites were studied.

2. MATERIALS AND METHODS

2.1 Materials

The Portland cement used in this work was cement CP II-Z-32 RS (resistant to sulfates and pozzolan), sold commercially by Votorantim Cement (Brazil). Portland cement is composed of 76-94% of clinker + calcium sulfate (gypsum), 6-14% of pozzolanic material and 0-5% of carbonate. The carbonate content should be at least 85% calcium carbonate ($CaCO_3$). It is cement for general use, specifically when moderate sulfate resistance or moderate heat hydration is desired, to work with aggressive medium and manufacturing cement mortar lining. The samples *in natura* of coir pith particles (30.7% lignin, 35.6% cellulose and 33.7% hemicellulose) [2] were obtained from Indufibras Indústria de Fibras Ltda. (Brazil), and refers to the waste produced after the coconut fibers industrialization, going through different washing and drying processes.

2.2 Sample preparation

Initially, the coir pith particles were submitted to natural drying for 120 hours. At that time was performed the processing of coir pith particles; these were subjected to the comminution process in a ball mill for 60 minutes, then the samples were classified in a series of sieves according to ASTM C33/ C33M-13 to get a particle size less than 0.3 mm. Finally, the coir pith particles were dried in an oven for 24 hours at 65 ± 5 °C until a constant weight was obtained.

Cement paste (Cp) was used as reference: 100% cement with a water-cement ratio of 0.30, without add coir pith or mineral aggregates. Two composites were produced: The first composites with coir pith particles *in natura* (Cnat): which has 100% cement with 10% coir pith particles with relating 1:0.10 (cement-coir pith particles) and a water-cement ratio of 0.75 (this value of water-cement ratio is used due to the high water absorption capacity of the coir pith particles, and to improve the composites workability). In addition, the second was cement-coir pith particles composites treated with Na_2CO_3: in this composite, the relation cement-coir pith particles and the ratio water-cement were kept the same, the treated with Na_2CO_3 consisted in mixing in the water used a Na_2CO_3 solution with concentration 0.1 mol/L.

The mixing process was adapted from OLORUNNISOLA [14] and BRASILEIRO *et al.* [2]. Cement

and coir pith particles were mixed on a beater with 5 liters capacity for 1 min at low-speed (140 rpm). Deionized water was added and mixed for 1 minute on low-speed (140 rpm). Finally, the composites were mixed for 2 minutes at high-speed (285 rpm). To produce the samples, stainless steel molds were used with internal dimensions 40 mm x 40 mm x 40 mm and 20 mm x 20 mm x 80 mm filled into two layers, with each layer put in a vibrating table for 5-15 sec and were covered with a glass plate. The samples were kept in the molds for 24 hours at laboratory ambient temperature of 23 ± 2 °C and relative humidity 65 ± 5 %. For compressive strength testing, four samples were assigned with dimensions of 40 mm x 40 mm x 40 mm. In addition, four samples with dimensions of 20 mm x 20 mm x 80 mm were used for three-point bending test and physical tests.

2.3 Curing process

For composites treated with Na_2CO_3 four curing conditions were employed in this study; wet cure (Cwet), dry curing (Cdry) and accelerated carbonation treatment more wet cure (Ccarbw) and more dry cure (Ccarbd). To the wet cure (Cwet), after unmolding, the specimens were immersed in deionized water for 27 days in a closed container (to allow saturation of water) in the laboratory with a temperature of 23 ± 2 °C, the same cure conditions was using for Cnat composites and cement paste Cp. For dry cure (Cdry), immediately after un-molding, the samples were covered in a PVC film and in an aluminum foil, and finally were transferred into a desiccator and subjected to a vacuum. For the curing conditions with accelerated carbonation treatment, the set-up and procedure consisted of a chamber of accelerated carbonation of polypropylene (PP), with a volumetric capacity of 56 liters. This chamber was hermetically sealed and adapted to a vacuum pump HP 1/4 New pump with flow speed between 54 to 58 L/min, and connected to the carbon dioxide gas cylinder, type ALS with contain 15 kg and pressure 58.3 kgf/cm^3, and the minimum purity of 99.999%. To keep the process of CO_2 injection into the chamber used a pressure regulator type LDS-CO2/N2 O-120. With the vacuum pump was left the chamber in a vacuum and removed the air inside it, and then was swollen the carbon dioxide, to keep up a flow of 100 ml/min for about 50 minutes, the process was repeated every 12 hours until 48 hours of cure. The Anhydrous silica gel was placed inside the chamber to remove the percentage of water evaporated from the test and control samples relative humidity. For monitoring the relative humidity and temperature variations inside the chamber, a hygrometer was placed in the chamber and recorded variations in temperature and humidity, once every hour during the healing process, within the carbonation chamber, a controlled environment was maintained at 25 ± 2 °C and 65 ± 5% temperature and relative humidity, respectively. The CO_2 healing process is illustrated in Figure 1.
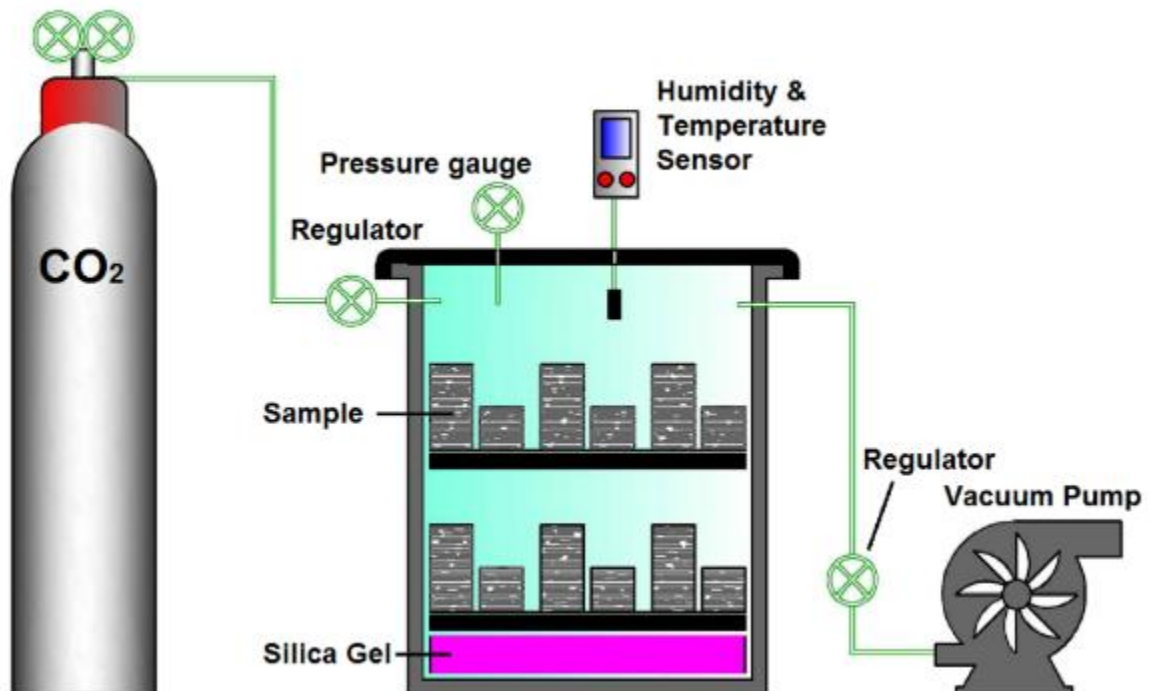
Figure 1: Illustration of the set-up for CO_2 curing of samples.

After completing time inside the chamber 4 samples were placed in a wet cure (Ccarbw) and 4 samples were wrapped with a thin PVC film and an aluminum foil, were then placed into a desiccator that was subjected to conditions vacuum (Ccarbd), in both conditions for 25 days, and thus complete the 28-day healing period for all samples.

2.4. Test method

2.4.1 Mechanical Tests

The mechanical tests were performed after 28 days of curing using INSTRON universal testing machine, model 3367. For compressive strength testing (CS), a 30 kN load cell and a rate of 1.0mm/min were used, according to ASTM C109/C109M-11. The three-point bending test was employed to evaluate the modulus of rupture (MOR), the modulus of elasticity (MOE) and specific energy (SE) of the samples. Using 5 kN load cell with a constant a deflection rate of 0.5 mm/min and 50 mm span, according to ASTM C348-08. The specific energy (SE) was defined as the energy absorbed during the flexural test, divided by the cross-sectional area of the specimens. The absorbed energy was obtained by integration of the area under the load-deflection curve at the point corresponding to a reduction in load carrying capacity to 30% of the maximum attained [1, 15].

2.4.2 Physical Tests

The physical properties of the samples as bulk density (BD), water absorption (WA) and apparent porosity (AP) were determined using the same procedures as ASTM C948-81(2016). The samples were placed for 24 hours in an oven at 100 ± 5 °C to obtain the dry weight (Wd); They were then immersed in water for 24 hours. After this time, they were weighed on an analytical balance to obtain the water-immersed weight (Wi). For the saturated weight (Ws), the surface water of the specimens was removed with absorbent paper. These properties were calculated using the formulas (1), (2) and (3)

$$BD \ (g/cm^3) = \frac{Wd}{Ws-Wi} \tag{1}$$

$$WA \ (\%) = (Ws - Wd) \times \frac{100}{Wd} \tag{2}$$

$$AP \ (\%) = (Ws - Wd) \times \frac{100}{Ws-Wi} \tag{3}$$

The true density of the coir pith particles was determined using helium pycnometry (Micromeritics AccuPyc II 1340).

2.4.3 Materials characterization

XRD analyses were conducted using a SHIMADZU diffractometer (XRD-6000), operating in scan mode, with Cu-Kα radiation (λ = 1.5418 A) and nickel filter with a voltage of 40 KV and 30 mA, scan rate 2°/min at 2θ (10-60°). The identification of mineral phases was obtained by comparison of X-ray diffractograms of the samples in the database of the Joint Committee on Powder Diffraction Standards-International Center for Diffraction Data (JCPDS-ICDD). The crystallinity index (CrI) of coir pith particles was calculated following empirical Segal method (modified by FRENCH in 2014 [16]) using equation (4):

$$CrI\% = \left(\frac{I_{200}-I_{am}}{I_{200}}\right) \times 100 \tag{4}$$

Where I_{200} is the maximum intensity (counts in units) of the crystalline phase peak 2θ = 22.01°. While I_{am} is the peak intensity of the amorphous phase at 2θ = 17.87°.

The cement hydration process can be evaluated by measuring the loss of mass after 28 days of the composite at 900 °C. The thermal analysis (TG/DTG) was performed in the simultaneous thermal analysis instrument NETZSCH STA 449 F1 JUPITER. The experimental conditions were performed under a nitrogen gas flow of 40 ml/min, the temperature range of 25-900 °C at a heating rate of 10 °C/min. The calcium hydroxide (CH) and calcium carbonate (CC) content were estimated from the measured mass loss in the TGA curve between the initial and final temperatures of the peaks of DTG. Agree with the reactions 5 and 6 [17]:

$$Ca(OH)_{2(s)} \rightarrow CaO_{(s)} + H_2O_{(g)} \tag{5}$$

$$CaCO_{3(s)} \rightarrow CaO_{(s)} + CO_{2(g)} \tag{6}$$

Where the molecular weight of $Ca(OH)_2$, CO_2 and H_2O and $CaCO_3$ are 74 g/mol, 44 g/mol, 100 g/mol, and 18 g/mol, respectively. The amounts of CH and CC were estimated using the percentage mass loss of the TGA curve, during the dihydroxylation (L_1) and decarbonation (L_2), in equations 7 and 8[17]:

$$\%CH = L_1 * \frac{74}{18} = 4{,}11 * L_1 \tag{7}$$

$$\%CC = L_2 * \frac{100}{44} = 2{,}27 * L_2 \tag{8}$$

The degree of carbonation from the amounts of calcium hydroxide (CH) and calcium silicate hydrate (C-S-H) was calculated from the percentage of calcium hydroxide and calcium carbonate of samples carbonated and samples non-carbonated determined by the TG curves [18]. The initial amount of CH ($CH_{INITIAL}$) which was carbonated can be calculated from equation (9) [18], this one was estimated by subtracting the %CH of carbonated composite from %CH of non-carbonated composite.

$$\%CH_{INITIAL} = \%CH + \frac{\%CC*74}{100} = \%CH + (0{,}74 * \%CC) \tag{9}$$

Considering the degree of carbonation as the amount calculated in %CC from the %CH, then the degree of carbonation was estimated from the amount of CH carbonated, according to equation 10,

$$\%CC = \%CH * \frac{100}{74} = 1{,}35 * \%CH \tag{10}$$

In addition, it is possible to estimate the %CC formed from the %C-S-H. According to Borges et al [17], the carbonates formed by C-S-H percentages are equal to the total amount of carbonates present after accelerated carbonation subtracting the carbonates formed from the calcium hydroxide (CH).

Micrographs were obtained using a scanning electron microscope JSM 5700 JEOL coupled with an energy dispersive spectrometer X-ray, using an accelerating voltage of 15 kV, working distance 14 mm and standard SB (secondary electron detection) mode. Previously, the samples were obtained from the surface of the fracture after the three-point bending test with a frontal area and a thickness of approximately 1 cm^2 and 5 mm, respectively and were coated with gold and were fixed with a double-sided tape of carbon.

3 RESULTS AND DISCUSSION

3.1 Characterization of coir pith particles

The coir pith particle used in this work is defined as a fine aggregate based on the particle size distribution while remaining in the area of the fine aggregates for concrete and mortar according to ASTM C33/C33M-13. The particle size distribution of coir pith is shown in Figure 2(a). After the grinding process of the particles, the fineness modulus reduces 2.56 to 1.57, which indicates that the coir pith particles passed relatively from an aggregate of medium fineness (2.0-3.0) to a fine aggregate (< 2.0), keeping particles in fine aggregate conditions, and the purpose of the grinding was to get a greater percentage of particles < 0.30 mm. The nominal maximum size remained at 2.4 mm. The true density of the coir pith particles is 1.6832 ± 0.0008 g/cm^3, obtained by pycnometric analysis.

Table 1 shows the elemental compositions estimated of the points analyzed with EDS for the coir pith particle presented in Figure 2c. In this table, can be seen the high percentage by weight of the elements C and O, that means the coir pith particle is composed mainly of organic matter, almost in their entirety. The presence of Si, Al, and Fe suggests that the particles of coir pith can be used as reinforce in cement-based composites [2,19], similar behavior found by BRIDGET *et al*. [6] in lignocellulosic materials, and could depend on the origin of the materials.

Table 1: Elemental chemical composition estimated for the coir pith particles (SEM-EDS).

Points	Detection of chemical elements (% by weight)					
	C	O	Al	Si	Ca	Fe
1	34.28	59.83	1.55	1.60	1.69	1.05
2	35.43	56.33	4.11	1.41	1.23	1.49

The X-ray diffractogram of coir pith particles used in this study is shown in Figure 2(b), being predominantly amorphous in structure assigned to hemicellulose and lignin. It shows the peak associated with the crystalline part that corresponds to the crystallographic plane (200) cellulose I ($2\theta = 22.01°$) and another around $2\theta = 17.87°$, corresponding to the amorphous fraction, typical of lignocellulosic material. The most intense peaks or more crystalline phases are related to the quartz or silicate commonly found in natural fibers [2,20]. The crystallinity index (CrI) of coir pith particles, calculated by equation 4 was 20.3%, it is lower than found in coconut fibers *in nature* (38.9%) [4].

Figure 2(c) shows the morphology of coir pith particle after the grinding process. The particles have a rough surface, roughened and exfoliated structures consisting of superposed plates similar to a crumpled sheet of paper [2]. A coarser morphology and increased roughness of surface have been reported as an advantage in manufacturing cement composites, improving particle-matrix interaction [19].
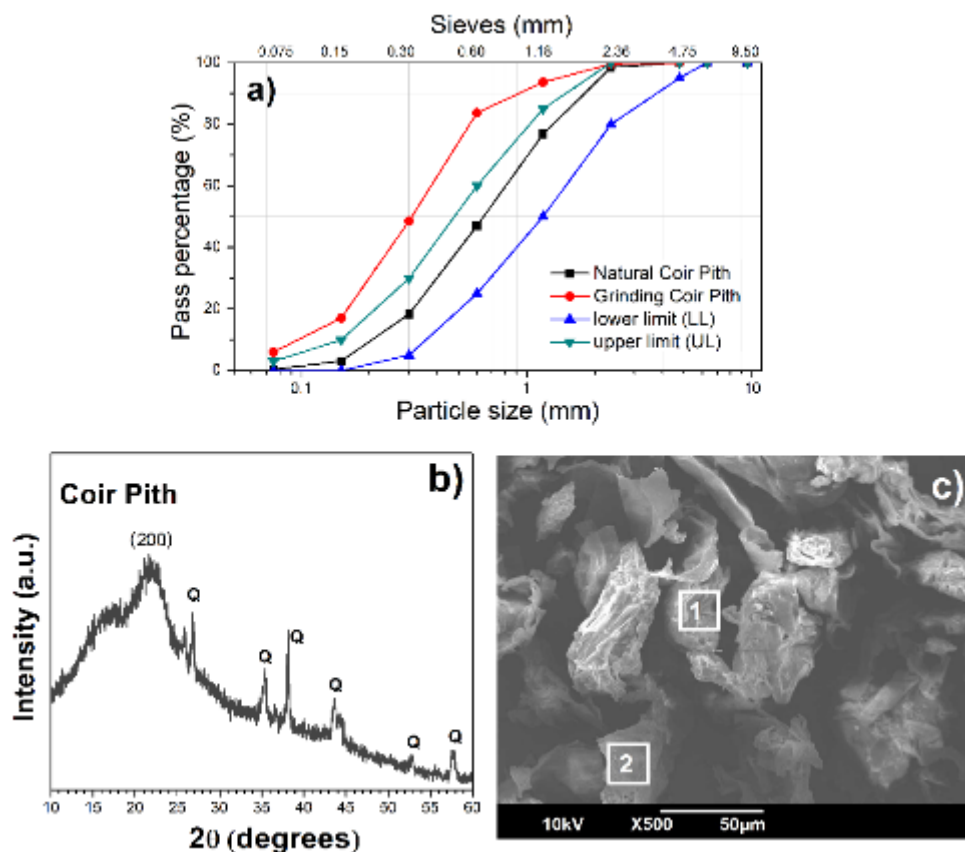
Figure 2: (a) Particle size distribution of the as-received coir pith and grinding coir pith. (b) Diffraction patterns X-ray of the coir pith particles, where: Q = quartz (JCPDS ICDD, 791910) and (c) scanning electron microscopy images of coir pith particles after the grinding process.

3.2 Carbonation process

In a fully hydrated process, Portland cement accounts for about 70% of hydrated calcium silicate (C-S-H), 20% $Ca(OH)_2$ and 10% calcium aluminosulfates (AFt and AFm) [21]. C-S-H is a very porous product with a large specific surface area and can absorb and release water during wetting and drying, leading to expansion and shrinkage of the hardened composite [21]. Some products after curing with CO_2 are $CaCO_3$ and silica gel [22], according to the following equations:

$$3CaO \cdot SiO_2 + 3CO_2 + \mu H_2O \rightarrow SiO_2 \cdot \mu H_2O + 3CaCO_3 \tag{11}$$

$$2CaO \cdot SiO_2 + 2CO_2 + \mu H_2O \rightarrow SiO_2 \cdot \mu H_2O + 2CaCO_3 \tag{12}$$

Figure 3 shows of fracture surfaces and a visual assessment of the phenolphthalein test using 1%

phenolphthalein solution, after 28 days of wet curing for carbonated composites (Ccarbw), non-carbonated (Cwet) and cement paste (Cp). As shown in Figure 3b, the non-carbonated sample (Cwet) and cement paste (Cp) show violet coloration after visual evaluation with a 1% phenolphthalein solution, the high violet color intensity is given as a result of a pH of the matrix between 10 and 12 [9]. The pH value of the water in common concrete or mortar pores normally exceeds 13 [23]. The high alkalinity occurs due to the calcium hydroxide $Ca(OH)_2$ formation during the cement hydration and is responsible for the vegetable materials degradation in cement composites [1]. However, $Ca(OH)_2$ can disappear gradually through the combination of CO_2 to form $CaCO_3$. This reaction decreases the alkalinity of the water in the pores, reducing the pH value to values close to 9 [23] because the alkaline medium degrades the lignocellulosic particles, then the accelerated carbonation could result in improving the cement composites durability.

In the carbonated samples at early cure age, a colorless area was observed on the fracture surface that penetrates between 3 mm to 5 mm from the surface, as shown in the visual evaluation with a phenolphthalein solution at 1% (Figure 3). Which mean that the carbonation process neutralizes the alkaline medium of the cement matrix that was more exposed to the medium with CO_2. This occurred because of the CO_2 reaction with the $Ca(OH)_2$ in the cement matrix, resulting in the calcium carbonate formation. Observing the carbonation penetration capacity in the samples, it could be said that the technique would have a good application in cement-lignocellulosic material panels, as shown by the results obtained in previous works where cement panels were made with sugarcane bagasse was cured by accelerated carbonation [9]. The phenolphthalein technique presents a quick result in the area that has carbonated most intensely, becoming colorless the carbonated region and purple color the non-carbonated region. However, a zone between the transitions of colors, where the pH values are between 9 and 13.5 cannot adequately evaluate with this technique.
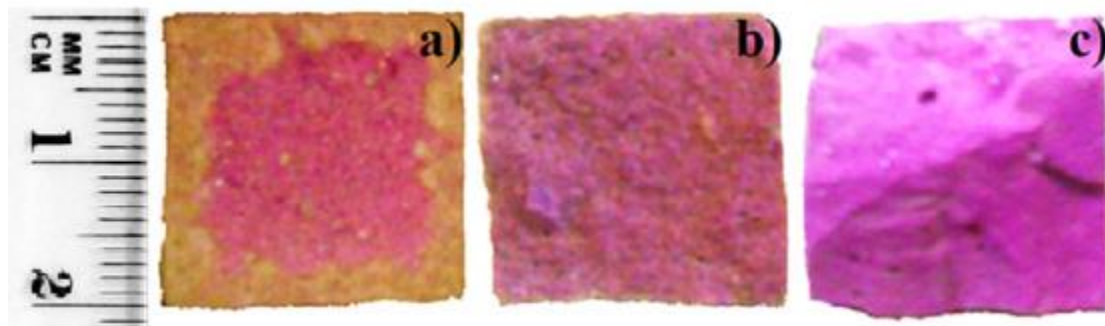
Figure 3: Visual assessment of fracture surfaces with 1% phenolphthalein solution, after 28 days of curing, for a) carbonated sample + wet cure (Ccarbw), b) only wet cure (Cwet) and c) cement paste (Cp).

After completion of the reactions between CO_2 and cement clinker, the percentage mass of $CaCO_3$ can be up to 75% based on CaO content of the cement. $CaCO_3$ is a crystalline product and exhibits excellent dimensional stability. In addition, the main cement binding component, calcium-hydrate silicate (C-S-H), could be decalcified by prolonged exposure to atmospheric CO_2, eventually becoming a silica gel (SiO_2) in the process and, as a result, losing its bonding capacity [23]. Although silica gel can also absorb and release water during wetting and drying processes, the silica gel percentage is lower than the $CaCO_3$ [21]. In order to understand the effect of CO_2 on cement hydration products, an analysis thermogravimetric of the samples was performed.

Figure 4 shows the TG and DTG curves of carbonated and non-carbonated composites for different curing conditions. According to the literature [1,18, 23-25] mass loss among the endothermic peaks 400-500 °C corresponds to dehydroxylation of $Ca(OH)_2$ and a peak between 600-750 °C corresponds to decarbonation of $CaCO_3$. The weight loss at 100 °C is associated with dehydration of water pores. The thermal decomposition of particles of coir pith occurs among the temperature the range between 295 and 370 °C.
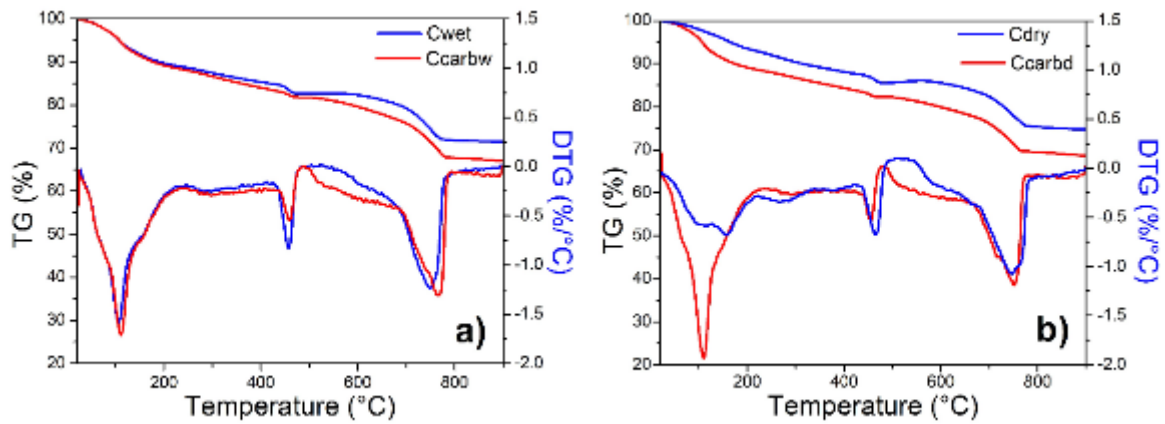
Figure 4: TG/DTG curves of the non-carbonated (Cwet and Cdry) and carbonated (Ccarbw and Ccarbd) composites at 28 days, (a) saturated cure and (b) dry cure.

The weight loss data for the TG curves are present in Table 2 for carbonated and non-carbonated composites subjected to dry and wet curing conditions, using the equation 7 and 8. Non-carbonated composite (Cdry and Cwet) showed a mass loss of about 10% at the peak near 700 °C, but the composites that were subjected to accelerated carbonation during the first hours of curing and after placed in saturated wet cure (Ccarbw) showed a mass loss around 14%, which means a higher $CaCO_3$ (CC) content on cement-coir pith particle composite.

Table 2: Data from TG analysis of the non-carbonated and carbonated composites after 28 days.

| Composites	Cure Condition	Loss of mass (%)
	Dry cure	
Cdry	CH	1.63
	CC	9.90
Ccarbd	CH	0.84
	CC	12.63
	Wet cure	
Cwet	CH	1.86
	CC	10.66
Ccarbw	CH	0.96
	CC	13.92

$CH=Ca(OH)_2$, $CC=CaCO_3$

Table 3 shows an estimate of the degree of carbonation from C-S-H (using equations 9 and 10), in a process is known as secondary carbonation, where the decalcified C-S-H is becoming CC and S-H (hydrated silicate), while the $Ca(OH)_2$ (CH) content is reduced or inaccessible [18]. The high porosity of the cement-coir pith particle composite promote a constant diffusion of the CO_2, and CH content is reduced more easily, allowing the decalcification of C-S-H [24]. The carbonation process during the early curing ages leads to reduction alkalinity of the matrix, which helps reduce the degradation of the cellulose and non-cellulosic constituents present in the coir pith particles. Despite the results of thermogravimetric analysis, this method is not completely exact, since it is necessary to take various conditions, but is useful for a quantified estimate of the effects of carbonation of the composites subject to cure with CO_2 at accelerated conditions. The main hydration product of the Portland cement paste is the C-S-H, comprises about 70% of cement paste [21], this is responsible for most of the properties of the hardened composite, for that reason, it is important to estimate the percentage of carbonates formed from C-S-H.

Table 3: Estimation of the extent of carbonation of C–S–H from TGA data, the non-carbonated and carbonated composites after 28 days.

Cure Condition	Non-carbonated composite			Carbonated composite				
	CH from TG (%)	CC from TG (%)	Initial calculation CH (%)	CH from TG (%)	CC from TG (%)	Amount carbonated of CH (%)	Expected CC from carbonating CH (%)	Carbonates formed by C–S–H (%)
Dry cure	6.70	22.50	23.35	3.45	28.70	19.90	26.89	1.82
Wet cure	7.65	24.23	25.57	3.95	31.64	21.63	29.23	2.41

The XRD patterns of carbonated and non-carbonated composites (Figure 5), show significant mineralogical changes in phases formed during the hydration process of the cement-based matrix, particularly in portlandite (Ca(OH)$_2$) and calcite (CaCO$_3$). The carbonation during the early cure age resulted in a decrease of the most characteristic peaks of portlandite (2θ = 18.10° and 2θ = 34.12°) and an increase in the calcite main peak (2θ = 29.48°). The XRD results confirm that there was a CO$_2$ absorption in the carbonated composite, as demonstrated in the TGA data, a fact also noted by earlier research [1,9]. Some other crystalline phases of the hydration product in the cement matrix are not identified in the carbonated composite, possibly have been decomposed because of the cure with CO$_2$ [24]. Previous works have managed to relate the intensities transition of the main peaks of portlandite and calcite to find the progress of the carbonation depth as a time function in the cement-based matrix [26].
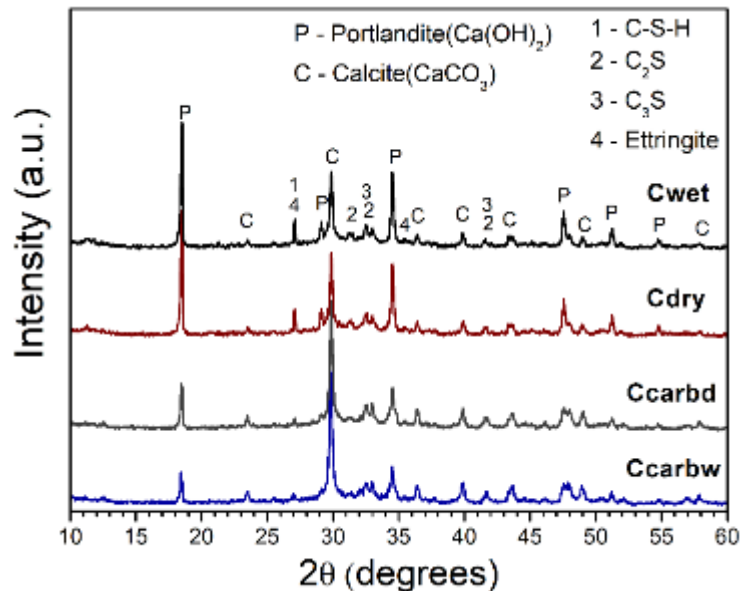
Figure 5: X-ray patterns from the non-carbonated and carbonated composites after 28 days, where: C=calcite or calcium carbonate, CaCO$_3$, (JCPDS-ICDD, 240027); P=portlandite or calcium hydroxide, Ca(OH)$_2$, (JCPDS-ICDD, 040733).

### 3.3 Mechanical and physical tests

Table 4 shows the performance of cement-based composites based on the results of compressive strength (CS), modulus of rupture (MOR), modulus of elasticity (MOE) and specific energy (SE) after 28 days of curing. Initially, the best results were observed in the composites treated with an alkaline solution of Na$_2$CO$_3$ in comparison to composites with particles *in natura* (Cnat). With respect to their chemical characteristics, in water the Na$_2$CO$_3$ forms carbonic acid (H$_2$CO$_3$) and OH-ions, these ones behaves as a buffer solution consisting of H$_2$CO$_3$ and sodium bicarbonate (NaHCO$_3$), turning the alkaline pH of the medium in around 12 [27]. The alkaline treatment could be most effective for removal of amorphous components present in the particles of coir pith such as hemicellulose, lignin, and pectin and partially could be increasing the crystallinity index of vegetable fibers [6,27]. The *in natura* coir pith particles are constituents for 35.6% cellulose and 64.4% non- cellulose (30.7% lignin and 33.7% hemicellulose) [2], the amount of cellulosic and non-cellulosic constituents in a vegetal fiber or particle influences the microstructure and physico-mechanical properties of cement-based composites [6]. When vegetal particles are integrated into the cement matrix could be responsible for the delay of cement hydration reaction in composites materials [28]. The XRD peaks

attributed to hydration products like ettringite or C-S-H do not appear or present low intensities in the composites after 28 days of cure (Figure 5), compared with XRD patterns from cement pastes without the addition of vegetal material where these peaks are presents [2,28].

**Table 4:** Mechanical characterization of the cement composite specimens at 28 days.

Specimens	CS (MPa)	MOR (MPa)	MOE (MPa)	SE (J/m^2)
Cp	29.81 ± 4.95	11.83 ± 1.50	1210.49 ± 116.15	408.26 ± 91.27
Cnat	4.35 ± 0.28	2.5 ± 0.23	220.27 ± 42.94	128.81 ± 16.27
Cwet	5.53 ± 1.04	2.79 ± 0.29	292.44 ± 35.38	105.94 ± 14.70
Cdry	5.35 ± 0.64	2.15 ± 0.26	155.03 ± 13.07	156.88 ± 2.38
Ccarbw	7.43 ± 0.43	3.47 ± 0.14	415.05 ± 39.97	133.43 ± 11.81
Ccarbd	6.10 ± 0.88	2.08 ± 0.10	181.36 ± 53.98	107.37 ± 17.57

The Figure 6 show the typical load-deflection curves under three-point bending flexural test). The incorporation of coir pith particles in the cement matrix reduces the modulus of rupture (MOR) when compared with the value corresponding to cement paste Cp, the reduction also leads to a decrease in the value of the toughness of the composites, since toughness corresponds to the integration of the area below the load-deflection curve. Nevertheless, it was observed a ductility increase in composites with coir pith particles in comparison with the brittle fracture of the cement paste (Cp), ductility is the cement-based material capacity to experiment a viscoelastic deformation before rupture, from the flexural test. The flexure deflection was 800 µm and 240 µm for composite with coir pith particles in natura (Cnat) and Cement paste (Cp), respectively. The increased ductility for composites with coir pith particles is related to the texture of the particles which have soft, flexible and stretchable and can absorb energy when applied a load on them [2]. The failure mode was changed from brittle failure to a more ductile mode. The MOR decreased to a value of around 2.44 MPa for Cnat, compared to 11.83 MPa of Cp (about 80% higher than Cnat). The load in composites with coir pith particles decreased slowly, while the flexure deflection value increased due the crack propagation in cement-based composites may occur at low stress and is usually characterized by a slow propagation [29]. When the load-deflection curve is descending, the load was gradually reduced as shown in figure 6. However, an increase in ductility for composites with coir pith particles was observed compared to cement paste [29]. The ductility is superior for the Cnat composites with respect to the Cwet composites, in the Cwet composites a treatment with an alkaline solution of Na$_2$CO$_3$ was used, probably the alkaline treatment improved the crystallinity of the coir pith particles in the cement matrix, removing partially the amorphous fraction [6], thus increasing their MOR in 17% with respect to Cnat. In addition, an increase in MOR of 28% for Ccarbw compared with Cnat, showing that accelerated carbonation during the early cure age improve de mechanical properties.
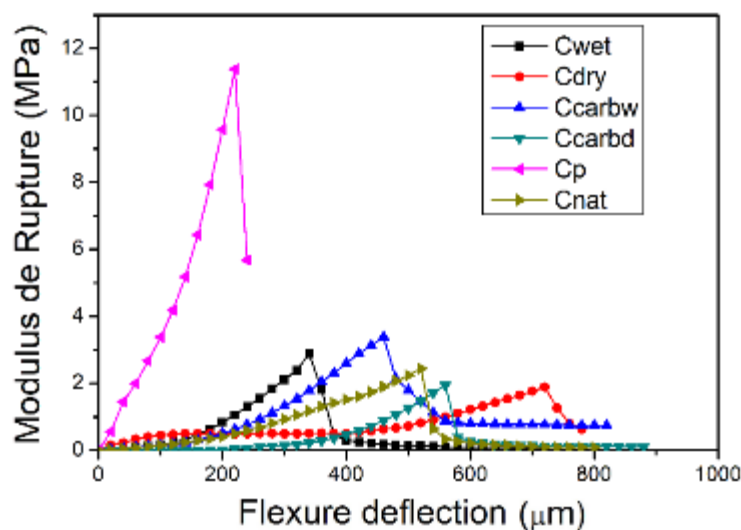
Figure 6: Typical load-deflection curves at 28 days, of the composites and cement paste under three-point bending flexural test.

Figure 7 shows the relationship between water absorption (WA) and apparent porosity (AP) with the bulk density (BD) of different composites. Physical properties presented are the result of microstructure and components produced in the cement-based matrix during the hydration process and carbonation. The composite Cnat showed the worst results in physical properties, forming materials more porous, less dense, which led to worse mechanical behavior. Putting the composites an environment rich in CO_2 during the first hours of curing leads to a reduction in the $Ca(OH)_2$ content and increase the $CaCO_3$, improving the particle-matrix interaction, due to $CaCO_3$ being more stable and denser than $Ca(OH)_2$, ettringite and C-S-H [1,25]. The $CaCO_3$ precipitates in the pores of the matrix structure and filling in gaps, swelling and blocking the water penetration due to a reduction in pore-scale [24], this explains the BD increase and AP reduction of carbonated composites. Increased AP and WA of the composites in dry cure condition, is because the natural process of hydration and carbonation produced by the environmental conditions was not properly completed. The samples remain isolated and sealed throughout the healing process. The physical properties contribute considerably to the mechanical behavior of composites.
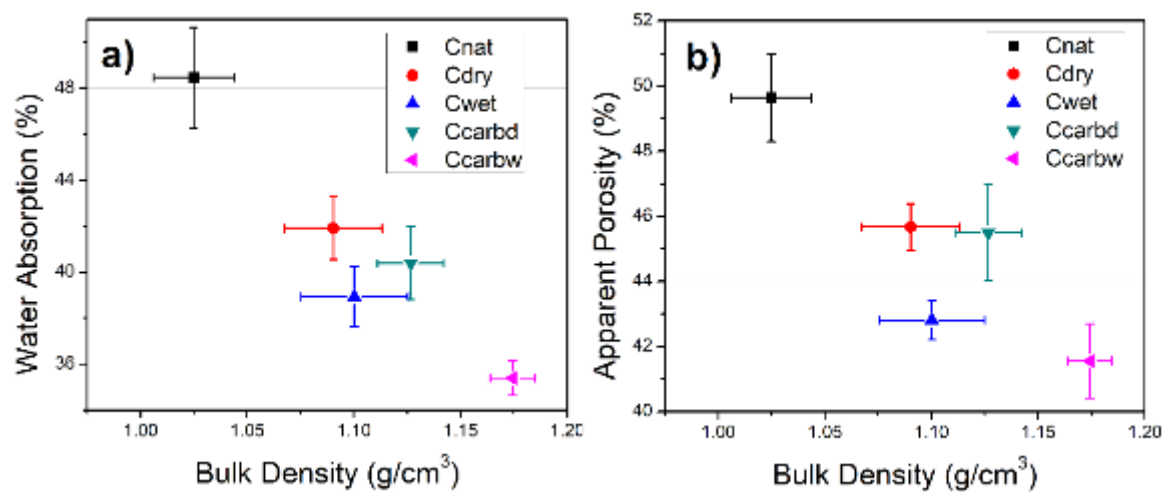

Figure 7: The correlation between bulk density and a) water absorption and b) apparent porosity of cement composites.

Figure 8 (a-d) shows the relationship between CS and SE with the bulk density (BD), also MOR and MOE with apparent porosity (AP) of the composite under different curing systems. The cement composites carbonated showed greater resistance to compression, increasing its resistance to 41.5% (7.43 MPa) for composites carbonated Ccarbw more resistant denser and, compared with the composite in nature Cnat of 4.35 MPa. The C-S-H and $CaCO_3$ precipitation occur after carbonation, with C-S-H being the most responsible for the gain in resistance [21,23]. In cement-based composites, the increasing rates of CS could vary for the following reasons; test age, aggregate vegetal material type, and carbonation grade [23]. The carbonation in cement-based composites causes a higher effect on the physical and mechanical properties if the reaction is in the first age of cure when the hydration products formed with lower intensity [23].

Improved MOR and MOE result was obtained for composites subjected to wet cure, which led to a decrease in porosity, especially for composites carbonated Ccarbw, with values of 3.47 MPa and 415.05 MPa for the MOR and MOE, respectively. These improved results are due to matrix densification, by hydration and carbonation processes. Additionally, the mechanical properties increases could be related to the joint effect of a cement matrix and coir pith particles, that could it mean that mechanical property is related to the mechanical strength of the matrix and the toughening mechanisms between the coir pith particles and the cement matrix [9]. The increases in mechanical properties show that the carbonated composites have improved the particle-matrix interaction; this interaction is affected by parameters such as the physical and chemical adhesion of particles in the matrix, orientation, and morphology of the particles. This transition zone (particle-matrix) has a region enriched with calcite [18], due to the reduced the $Ca(OH)_2$ content during the carbonation treatment in the first curing ages.

The specific energy (SE) values of the composite without carbonation Cnat and Cdry are 128.81 J/m^2

and 156.88 J/m^2, respectively. These composites, while enduring low loads, have greater deformation higher to 800 μm, this suggests that the coir pith particles was maintained in a less alkaline matrix and was remained a smooth transition in the particle-matrix area, allowing the energy dissipation in the post-fracture region, for this reason, the higher SE values. The carbonation treatment could be contributed to decreasing the fibers degradation, this degradation occurs by the easy movement of the pore water towards the cement matrix [18], for this reason, the composites carbonated (Ccarbw) show a WA and AP decrease (Figure 7) and additionally causes a slightly brittle fracture of the composite (Figure 6). SEM analyses were performed on the surface of fracture to better understand the interaction between the particles of coir pith and cement matrix.
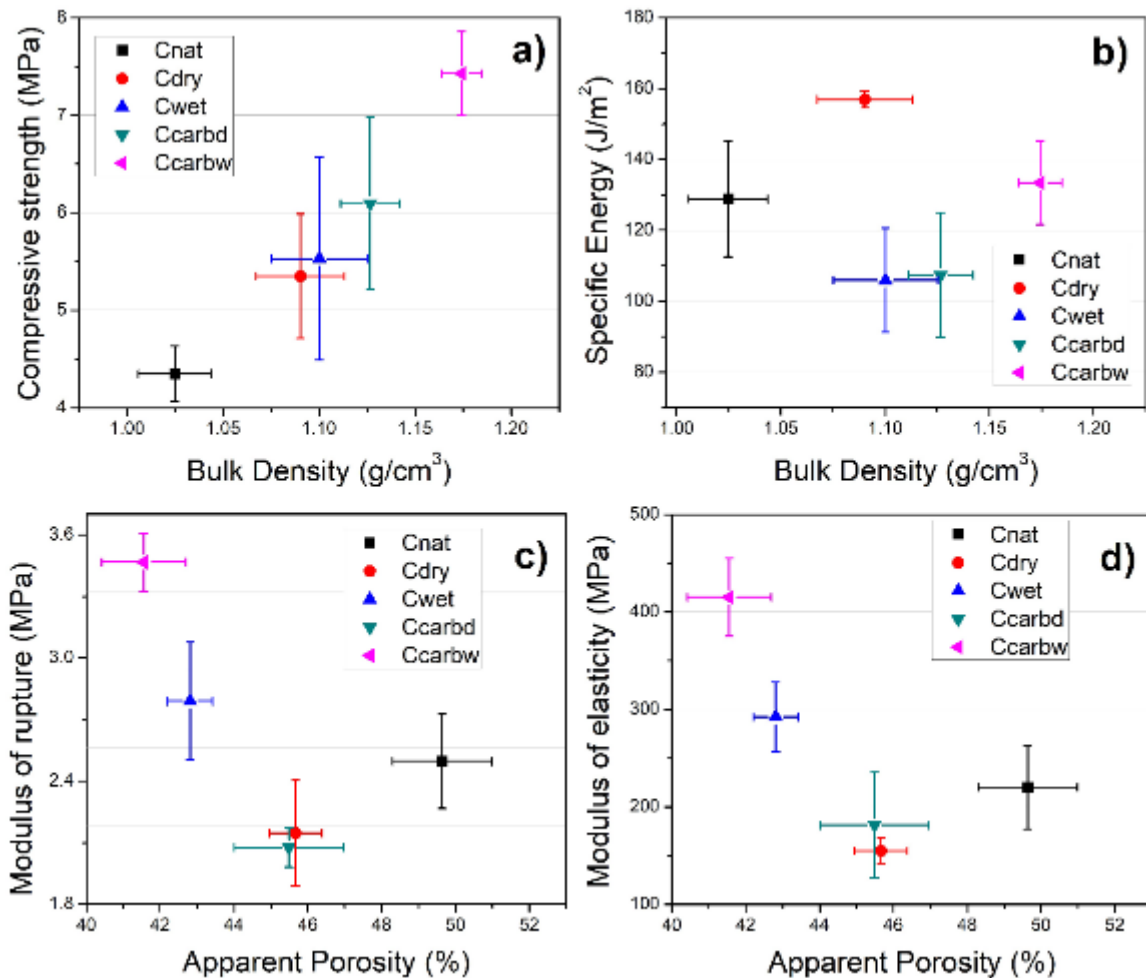
Figure 8: Values of mechanical properties vs. bulk density (BD): (a) compressive strength (CS) and (b) specific energy (SE). Also, mechanical properties vs. apparent porosity (AP): (c) modulus of rupture (MOR) and (d) modulus of elasticity (MOE).

The micrographs shown in Figure 9 were obtained by SEM in the secondary electron mode and were accompanied by EDS measurement. The surface of fracture was evaluated after mechanical test performed with 28 days curing of the non-carbonated composite Cwet and carbonated composite Ccarbw. The analysis of these micrographs allows observation of the cement morphologies developed after exposure to accelerated carbonation, and their impact on the interface between the coir pith particles and the cement matrix. The micrographs in Figure 9(a) show needle forms probably ettringite, these needles are formed in the pores of the matrix and around the coir pith particles in non-carbonate composites Cwet (according to EDS results in Table 4). The needle formations are not observed for carbonated composite Ccarbw, as shown in Figure 9(b). The carbonated composite (Ccarbw) morphology was compact and formed by layered structures, probably related to the phases of CaCO$_3$, corroborating the results of thermal analysis TG/DTG, where the mass loss resulted in a lower concentration of Ca(OH)$_2$ than carbonated phases CaCO$_3$ and the resulting carbonates of the C-S-H.
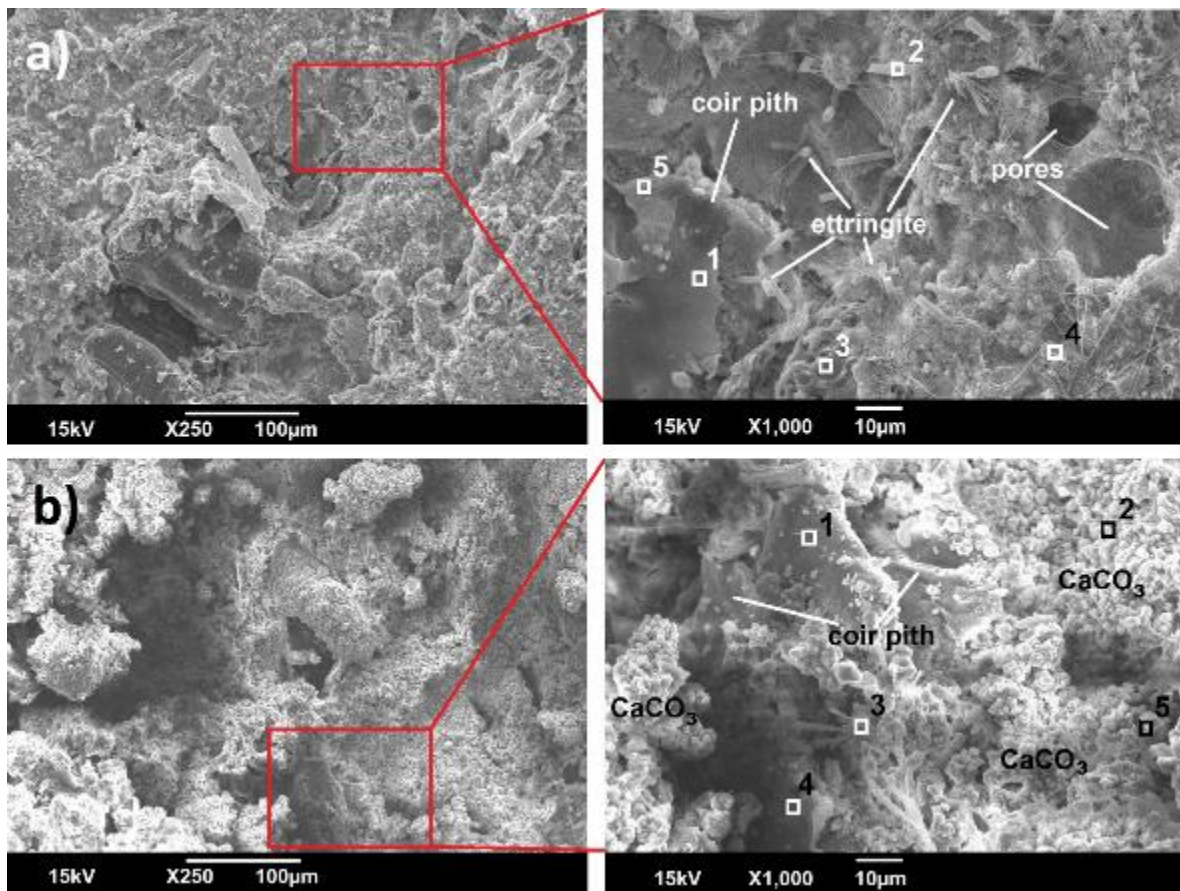
Figure 9: Scanning electron micrographs of the fracture surface of (a) non-carbonated composite (Cwet) and (b) carbonated composite (Ccarbw) at 28 days, with 250x magnification. EDS analysis points are highlighted, with 1000x magnification.

Table 5 shows an estimate of the chemical elements of the points analyzed with EDS. The increases in the weight percentage of calcium element (Ca) in the EDS analysis, mean an increase in accelerated carbonation rate and a reduction the free water content, increasing the CO_2 diffusion around the interface between the coir pith particles and the cement matrix and thus the calcium ions can be sequestered in the regions near this interface [18]. Calcium ions are highly movable in the cement hydration solution, causing hydration products accumulation in the interface between vegetable particles and cement matrix as $Ca(OH)_2$ and C-S-H [2]. When carbonation is applied during the first hours of cure, these hydration products are replaced by carbonates, as explained in the thermal analysis. The point with a high percentage of carbon and oxygen could be due to the coir pith particles presence since these particles are composed mainly of organic matter as seen in the EDS analysis of coir pith particles.

Table 5: Elemental chemical composition estimated for the non-carbonated and carbonated composites at 28 days (SEM-EDS).

Figure	Composites	Points	Detection of chemical elements (% by weight)								
			C	O	Na	Al	Si	S	K	Ca	Fe
Fig. 9(a)	Non-carbonated (Cwet)	1	18.04	51.82	0.00	1.20	6.59	0.00	0.00	18.90	3.45
		2	17.04	21.45	0.00	2.32	4.92	4.44	0.00	49.82	0.00
		3	3.59	55.00	0.00	0.44	5.18	0.00	2.30	27.13	6.36
		4	26.22	53.03	0.00	0.00	0.00	0.00	0.70	20.05	0.00
		5	17.89	57.54	2.67	0.00	0.00	2.08	0.00	19.83	0.00
Fig. 9(b)	Carbonated (Ccarbw)	1	10.32	28.87	0.00	0.00	6.16	0.00	1.83	52.82	0.00
		2	1.70	53.28	0.00	0.00	2.55	0.00	0.00	37.91	4.56
		3	7.73	43.19	0.00	1.43	0.00	0.00	0.00	47.64	0.00
		4	0.00	19.50	0.00	0.00	5.31	0.00	11.57	63.62	0.00
		5	3.35	52.42	0.00	0.00	2.75	0.00	0.00	41.48	0.00

4. CONCLUSIONS

Treatment of accelerated carbonation during the early cure age of cement-based composites, was an efficient treatment since it densified the matrix and preserved the coir pith particle decreasing the alkalinity of the cement matrix by reducing the $Ca(OH)_2$ concentration, demonstrating a good sequestering capacity of carbon dioxide.

The coir pith particles composites have a higher ductility, enduring longer charge before rupture, leading to a greater deformation. Coir pith particles have a higher ability to absorb energy during fracture, therefore, has higher values of specific energy, unlike the brittle fracture of cement paste (Cp).

The interaction between the decrease of $Ca(OH)_2$, and the increase of $CaCO_3$ content was discussed by results of thermal analysis and X-ray diffraction. At DTG curves, the surroundings peak 700 °C associated with the degradation of $CaCO_3$ (decarbonation process) shows greater mass lost for composite Ccarbw, these composites exhibit the highest content of carbonates formed from $Ca(OH)_2$ and C-S-H. With respect to the different curing conditions, the samples submitted to accelerated carbonation 48 h in a controlled environment followed by a wet cure (Ccarbw) presented an improvement in the mechanical properties obtaining a more densified matrix and with less porosity.

The analysis of the fracture surface by SEM micrographs for carbonated composite showed layered structures on its surface, probably $CaCO_3$, which was also confirmed by increasing the calcium content in the EDS analysis. The $CaCO_3$ precipitates in the pores of the cement matrix, filling in gaps, preventing the water infiltration, and density the cement matrix.

5. ACKNOWLEDGEMENTS

6. BIBLIOGRAPHY

[1] ALMEIDA, A. E. F. S., TONOLI, G. H. D., SANTOS, S. F., *et al.*, "Improved durability of vegetable fiber reinforced cement composite subject to accelerated carbonation at early age", *Cement & Concrete Composites*, v. 42, pp. 49-58, 2013.

[2] BRASILEIRO, G. A. M., VIEIRA, J. A. R., BARRETO, L. S., "Use of coir pith particles in composites with Portland cement", *Journal of Environmental Management,* v. 131, pp. 228-238, 2013.

[3] BELOUADAH, Z., ATI, A., ROKBI, M., "Characterization of new natural cellulosic fiber from Lygeum spartum L", *Carbohydrate Polymers,* v. 134, pp. 429-437, 2015.

[4] ROSA, M. F., MEDEIROS, E. S., MALMONGE, J. A., *et al.*, "Cellulose nanowhiskers from coconut husk fibers: Effect of preparation conditions on their thermal and morphological behavior", *Carbohydrate Polymers,* v. 81, pp. 83-92, 2010.

SUAZO, F.J.A.; CARREGOSA, J.D.C.; OLIVEIRA, R.M.P.B., *et al.*, revista Matéria, v.25, n.2, 2020.

[5] KARADE, S. R., "Cement-bonded composites from lignocellulosic wastes", *Construction and Building Materials,* v. 24, pp. 1323–1330, 2010.

[6] BRÍGIDA, A. I. S., CALADO, V. M. A., GONÇALVES, L. R. B., *et al.,* "Effect of chemical treatments on properties of green coconut fiber", *Carbohydrate Polymers,* v. 79, pp. 832-838, 2010.

[7] BOŁTRYK, M., PAWLUCZUK, E., "Properties of a lightweight cement composite with an ecological organic filler", *Construction and Building Materials,* v. 51, pp. 97-105, 1/31/ 2014.

[8] JUNIOR, A. N., FERREIRA, S. R., TOLEDO FILHO, R. D., *et al.*, "Effect of early age curing carbonation on the mechanical properties and durability of high initial strength Portland cement and lime-pozolan composites reinforced with long sisal fibres", *Composites Part B: Engineering,* v. 163, pp. 351-362. 2018.

[9] CABRAL, M. R., NAKANISHI, E. Y., FIORELLI, J., "Cement-bonded panels produced with sugarcane bagasse cured by accelerated carbonation", *Journal of Materials in Civil Engineering,* v. 30, pp. 04018103, 2018.

[10] CABRAL, M. R., NAKANISHI, E. Y., FIORELLI, J., "Evaluation of the effect of accelerated carbonation in cement–bagasse panels after cycles of wetting and drying", *Journal of Materials in Civil Engineering,* v. 29, pp. 04017018, 2017.

[11] RAMLI, M., KWAN, W. H., ABAS, N. F., "Strength and durability of coconut-fiber-reinforced concrete in aggressive environments", *Construction and Building Materials,* v. 38, pp. 554-566, 2013.

[12] TOLÊDO FILHO, R. D., GHAVAMI, K., ENGLAND, G. L., *et al.*, "Development of vegetable fibre-mortar composites of improved durability", *Cement & Concrete Composites,* v. 25, pp. 185–196, 2003.

[13] JERGA, J., "Physico-mechanical properties of carbonated concrete", *Construction and Building Materials,* v. 18, pp. 645-652, 2004.

[14] OLORUNNISOLA, A. O., "Effects of husk particle size and calcium chloride on strength and sorption properties of coconut husk–cement composites", *Industrial Crops and Products,* v. 29, pp. 495-501, 2009.

[15] TONOLI, G. H. D., RODRIGUES FILHO, U. P., SAVASTANO JR, H., *et al.*, "Cellulose modified fibres in cement based composites", *Composites: Part A,* v. 40, pp. 2046–2053, 2009.

[16] FRENCH, A.D., "Idealized powder diffraction patterns for cellulose polymorphs", *Cellulose*, v. 21, pp. 885-896, 2014.

[17] BORGES, P. H. R., COSTA, J. O., MILESTONE, N. B., *et al.*, "Carbonation of CH and C–S–H in composite cement pastes containing high amounts of BFS", *Cement and Concrete Research,* v. 40, pp. 284-292, 2010.

[18] SANTOS, S. F., SCHMIDT, R., ALMEIDA, A. E. F. S., *et al.*, "Supercritical carbonation treatment on extruded fibre–cement reinforced with vegetable fibres", *Cement & Concrete Composites,* v. 56, pp. 84–94, 2015.

[19] NARENDAR R., DASAN, K. P., "Chemical treatments of coir pith: Morphology, chemical composition, thermal and water retention behavior", *Composites Part B-Engineering,* v. 56, pp. 770-779, Jan. 2014.

[20] MACEDO, J. S., OTUBO, L., FERREIRA, O. P., *et al.*, "Biomorphic activated porous carbons with complex microstructures from lignocellulosic residues", *Microporous and Mesoporous Materials,* v. 107, pp. 276-285, 2008.

[21] SHI, C., WANG, D., HE, F., *et al.,* "Weathering properties of CO2-cured concrete blocks", *Resources, Conservation and Recycling,* v. 65, pp. 11-17, 2012.

[22] GOODBRAKE, C. J., YOUNG, J. F., BERGER, R. L., "Reaction of Hydraulic Calcium Silicates with Carbon Dioxide and Water", *Journal of the American Ceramic Society,* v. 62, pp. 488-491, 1979.

[23] ZHANG, D., GHOULEH, Z., SHAO, Y., "Review on carbonation curing of cement-based materials", *Journal of CO2 Utilization,* v. 21, pp. 119-131, 2017.

[24] PIZZOL, V. D., MENDES, L. M., FREZZATTI, L., *et al.,* "Effect of accelerated carbonation on the microstructure and physical properties of hybrid fiber-cement composites", *Minerals Engineering,* v. 59, pp. 101-106, May 2014.

[25] FRÍAS, M., GOÑI, S., "Accelerated carbonation effect on behaviour of ternary Portland cements", *Composites Part B: Engineering,* v. 48, pp. 122-128, 2013.

[26] CHANG, C. F., CHEN, J. W., "The experimental investigation of concrete carbonation depth", *Cement and Concrete Research,* v. 36, pp. 1760– 1767, 2006.

[27] LE TROEDEC, M., SEDAN, D., PEYRATOUT, C., *et al.*, "Influence of various chemical treatments on the composition and structure of hemp fibres", *Composites Part A: Applied Science and Manufacturing,* v. 39, pp. 514-522, Mar. 2008.

[28] SEDAN, D., PAGNOUX, C., SMITH, A., *et al.*, "Mechanical properties of hemp fibre reinforced cement: Influence of the fibre/matrix interaction", *Journal of the European Ceramic Society,* v. 28, pp. 183-192, 2008.

[29] DING, Y., YU, J. T., YU, K. Q., *et al.,* "Basic mechanical properties of ultra-high ductility cementitious composites: From 40 MPa to 120 MPa", *Composite structures,* v. 185, pp. 634-645, 2018.

ORCID

Franco Josué Amaya Suazo   https://orcid.org/0000-0001-9066-2902
João Domingos Covello Carregosa   https://orcid.org/0000-0001-8801-7939
Rosane Maria Pessoa Betânio Oliveira   https://orcid.org/0000-0002-2726-1863
Wilson Acchar   https://orcid.org/0000-0002-5585-1799